

Stabilization and Improvement of a Promising Influenza Antiviral: Making a PAIN PAINless

Aleksandar Antanasijevic,[†] Nicholas J. Hafeman,[‡] Smanla Tundup,[#] Carolyn Kingsley,[†] Rama K. Mishra,[§] Lijun Rong,[‡] Balaji Manicassamy,[#] Duncan Wardrop,[‡] and Michael Caffrey^{*,†}

[†]Department of Biochemistry & Molecular Genetics, University of Illinois at Chicago, 900 South Ashland Avenue, Chicago, Illinois 60607, United States

[‡]Department of Chemistry, University of Illinois at Chicago, 845 West Taylor Street, Chicago, Illinois 60607, United States

[#]Department of Microbiology and Immunology, University of Chicago, 920 East 58th Street, Chicago, Illinois 60637, United States

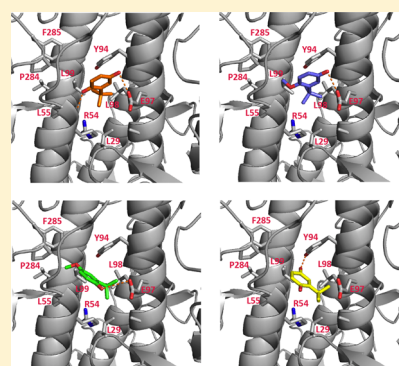
[§]Center for Molecular Innovation and Drug Discovery, Northwestern University, 2135 Sheridan Road, Evanston, Illinois 60208, United States

[‡]Department of Microbiology & Immunology, University of Illinois at Chicago, 835 South Wolcott, Chicago, Illinois 60612, United States

S Supporting Information

ABSTRACT: The viral envelope protein hemagglutinin (HA) plays a critical role in influenza entry and thus is an attractive target for novel therapeutics. The small molecule *tert*-butylhydroquinone (TBHQ) has previously been shown to bind to HA and inhibit HA-mediated entry with low micromolar potency. However, enthusiasm for the use of TBHQ has diminished due to the compound's antioxidant properties. In this work we show that the antioxidant properties of TBHQ are not responsible for the inhibition of HA-mediated entry. In addition, we have performed a structure–activity relationship (SAR) analysis of TBHQ derivatives. We find that the most promising compound, 3-*tert*-butyl-4-methoxyphenol, exhibits enhanced potency ($IC_{50} = 0.6 \mu M$), decreased toxicity ($CC_{50} = 340 \mu M$), and increased stability ($t_{1/2} > 48$ h). Finally, we have characterized the binding properties of 3-*tert*-butyl-4-methoxyphenol using NMR and molecular dynamics to guide future efforts for chemical optimization.

KEYWORDS: glycoprotein, hemagglutinin, molecular dynamics, NMR, TBHQ, viral entry



Hemagglutinin (HA) and neuraminidase (NA), which are viral membrane glycoproteins, play critical roles in influenza infection.¹ On the basis of antigenic properties, influenza strains are classified into subtypes of HA (H1–H18) and NA (N1–N11), with some strains presenting significant threats to human health.² For example, with a fatality rate of 3%, the H1N1 influenza pandemic of 1918 caused over 50 million deaths worldwide. Moreover, seasonal influenzas, including H3N2, are responsible for >500,000 deaths per year worldwide, despite improved vaccination efforts and better treatments.^{3,4} In addition, the recent outbreak of H7N9 in China, which exhibited fatality rates of >20%, is of very high concern.^{5,6} Current treatments for influenza include small molecules targeting NA and the M2 channel of influenza; however, circulating strains of influenza are exhibiting increased drug resistance.⁷ For example, almost all circulating influenza strains are resistant to M2 drugs. In addition, the 2008–2009 H1N1 strain exhibited ~100% resistance against Tamiflu,⁸ which targets NA. Moreover, some H7N9 strains of the recent outbreak have also developed resistance to Tamiflu.⁹ Consequently, influenza may now be considered as a drug-resistant pathogen. In summary, the unpredictable nature of

novel influenza outbreaks and the observed resistance to current therapeutics strongly argue that new therapeutic targets are urgently needed, particularly against newly emerging strains, such as H7N9, as well as seasonal strains such as H3N2.

HA, as well as the analogous glycoproteins of other enveloped viruses including Ebola, HIV, and MERS- and SARS-Coronavirus, promotes virus entry by first binding to a receptor and subsequent changes in conformation, resulting in fusion of the viral and target cell membranes.^{1,10–13} On the basis of the sequence, structure, and immunogenicity, HA falls into two phylogenetic groups.^{2,14} For example, H1 and H5 HA are members of group 1, and H3 and H7 HA are members of group 2. HA is synthesized as a precursor (HA0) in all cases and later cleaved to form a disulfide-linked complex composed of the receptor binding subunit HA1 and the fusion subunit HA2.¹ The critical nature of HA function renders it an attractive target for therapeutic intervention by small molecules, proteins, or antibodies designed to disrupt the binding or fusion steps of viral entry (i.e., binding or fusion inhibitors^{7,15–28}). In

Received: March 24, 2016

Published: July 25, 2016

the case of the fusion inhibitors, it is thought that they bind to the highly conserved stem loop region of HA2 and disrupt function by stabilizing the prefusion (i.e., neutral pH) conformation.^{22,24–27} Interestingly, the fusion inhibitors appear to operate in a group-specific manner.^{22,24–28} For example, inhibitors of group 1 HA, including H1 and H5, do not inhibit group 2 HA, including H3 and H7. Despite the clear potential of fusion inhibitors, there are no examples of FDA-approved small molecules that target HA. Consequently, inhibitors of HA function offer unique opportunities for treating influenza, including drug-resistant strains, for which resistance is to NA or M2 inhibitors and *not* HA.

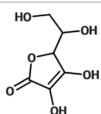
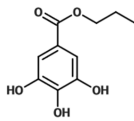
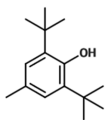
The small molecule *tert*-butylhydroquinone (TBHQ) is an example of a group 2 HA inhibitor with low micromolar IC₅₀ in pseudovirus and infectious virus assays.^{15,22,27} Interestingly, TBHQ is a FDA-approved antioxidant,²⁹ and thus its low toxicity makes it an attractive lead compound. However, the antioxidant properties of TBHQ diminish enthusiasm due to potential oxidation–reduction reactions (e.g., reduction of disulfide bonds) or covalent attachment to host proteins. Indeed, hydroquinone derivatives are generally considered to be pan assay interference compounds (PAINS), which promiscuously bind to targets and consequently should be removed from the “hit” list of industrial screens.^{30,31} In this work we first show that the antiviral properties of TBHQ are not related to oxidation–reduction reactions. We then describe the modulation of the TBHQ potential reactivity and the enhancement of the derivative’s antiviral activity through a structure–activity study. Finally, we use NMR and molecular dynamics to characterize the interaction between the most promising compound and H7 HA. In summary, we believe that the present work will renew interest in this class of molecules as potential therapeutic agents against influenza, as well as encourage a re-examination of previously discarded compounds designated PAINS in screens of other protein targets.

RESULTS AND DISCUSSION

TBHQ Inhibition Is Not Due to Its Antioxidant Properties. To test whether the antioxidant properties of TBHQ are related to its antiviral activity, we assayed the activity of three other common antioxidant food additives: ascorbic acid (compound 1), propyl gallate (compound 2), and 2,6-di-*tert*-butyl-4-methylphenol (compound 3), using an H7 HA-based pseudovirus entry assay.²⁷ In this assay, pseudovirus is prepared with the viral envelope protein of choice, H7 HA in the present case, contained on the background of the HIV core. In addition, we assayed compound activity against VSVG-mediated entry, an unrelated viral envelope protein, to assess specificity and cytotoxicity.²⁷ As shown in Table 1, the antioxidants exhibit little inhibition of HA-mediated entry (IC₅₀ > 10× that of TBHQ), which strongly suggests that TBHQ oxidizing properties are not responsible for its antiviral activity. Nonetheless, we note that the compound that exhibits measurable activity, compound 3 with IC₅₀ = 60 μM, is structurally closest to TBHQ (compound 4).

Structure–Activity Relationship (SAR) Analysis of TBHQ Hydroxyl Groups. Under physiological conditions of pH, temperature, and oxygen concentration, TBHQ (compound 4) undergoes a reversible oxidation to form *tert*-butylbenzoquinone (TBBQ), which forms the basis of its antioxidant properties.³² Thus, we compared the antiviral activity of TBHQ to that of TBBQ (compound 5). As shown in Table 2, compound 5 (the oxidized version of TBHQ) exhibits

Table 1. Antiviral Properties of Antioxidants

Compound Structure	Compound	H7 HA IC ₅₀ (μM)	VSVG CC ₅₀ (μM)
	1 Ascorbic acid	> 100	> 100
	2 Propyl gallate	> 100	> 100
	3 2,6-di- <i>tert</i> -Butyl-4-methylphenol	~ 60	> 100

little activity in the assayed concentration range, suggesting that one or more of the hydroxyl groups form critical interactions with HA. In the next step, we assayed the importance of the 1-hydroxyl and 4-hydroxyl groups of TBHQ to its antiviral activity. First, substitution of the 4-hydroxyl group with a methoxy substituent to form an anisole (compound 6) significantly attenuates inhibition of virus entry (Table 2), suggesting that the 4-hydroxyl group forms important contacts with HA. This notion is further supported by the decreased potency exhibited by compounds 7, 8, 9, and 10, in which the 4-hydroxyl group is substituted by hydrogen, methyl, ethyl, and bromo groups, respectively (Table 2). Next, replacement of the 1-hydroxyl group with a methoxy substituent to form an anisole (compound 11) improves the IC₅₀ by ~10×, suggesting that the 1-hydroxyl group is not critical and that the newly introduced O-alkyl group makes significant contacts with HA. Moreover, the importance of the 4-hydroxyl group is further supported by the observation that its substitutions in the most active anisole derivative (compound 11) by hydrogen, carboxylic acid, hydroxymethyl, amidyl, methylamidyl, and ethylamidyl groups (compounds 12, 13, 14, 15, 16, and 17, respectively) exhibit significantly decreased activity. Finally, to assay the potential to improve upon the methoxy substituent of compound 11, ethoxy, isopropoxy, isobutoxy, and *sec*-butoxy groups were substituted for the methoxy substituent (compounds 18, 19, 20, and 21, respectively). However, all four analogues exhibit significant loss in activity (Table 2), which underscores the importance of the methoxy substituent at this position.

In the next step, we tested the potency of 2-*tert*-butyl-4-methoxyphenol (compound 6) and 3-*tert*-butyl-4-methoxyphenol (compound 11), against infectious H3 influenza, which possesses another group 2 HA. As shown in Figure 1, compound 6 is relatively inactive, in agreement with the pseudovirus assay for H7 HA. In contrast, compound 11 exhibits an IC₅₀ = 4 μM (Figure 1), which is in relatively good agreement with the inhibition observed using the pseudovirus assay for H7 HA. Finally, we measured the cytotoxicity of compound 4 (TBHQ, the parent compound), compound 5 (oxidized TBHQ), compound 6 (inactive anisole derivative), and compound 11 (the most active anisole derivative). As shown in Figure 2, compounds 4, 6, and 11 exhibit CC₅₀ > 270 μM, with the anisole versions showing significantly less toxicity than the parent compound. Consequently, the selectivity index of compound 11 is >500.

Table 2. Antiviral Properties of TBHQ and Derivatives

Compound Structure	Compound	H7 HA IC ₅₀ (μM)	VSVG CC ₅₀ (μM)	Compound Structure	Compound	H7 HA IC ₅₀ (μM)	VSVG CC ₅₀ (μM)
	4 <i>tert</i> -Butylhydroquinone (TBHQ)	6	> 50		13 3-(<i>tert</i> -Butyl)-4-methoxybenzoic acid	> 50	> 50
	5 <i>tert</i> -Butylbenzoquinone (TBBQ)	> 50	> 50		14 (3-(<i>tert</i> -Butyl)-4-methoxyphenyl) methanol	10	> 50
	6 2- <i>tert</i> -Butyl-4-methoxyphenol	30	> 50		15 3-(<i>tert</i> -Butyl)-4-methoxybenzamide	> 50	> 50
	7 2- <i>tert</i> -Butylphenol	25	> 50		16 3-(<i>tert</i> -Butyl)-4-methoxy- <i>N</i> -methylbenzamide	> 50	> 50
	8 2- <i>tert</i> -Butyl-4-methylphenol	> 50	> 50		17 (3-(<i>tert</i> -Butyl)-4-methoxyphenyl) methanamine	30	> 50
	9 2- <i>tert</i> -Butyl-4-ethylphenol	> 50	> 50		18 3-(<i>tert</i> -Butyl)-4-ethoxyphenol	10	>50
	10 4-Bromo-2- <i>tert</i> -butylphenol	> 50	> 50		19 3-(<i>tert</i> -Butyl)-4-isopropoxyphenol	3	>50
	11 3- <i>tert</i> -Butyl-4-methoxyphenol	0.6	> 50		20 3-(<i>tert</i> -Butyl)-4-isobutoxyphenol	3	>50
	12 1-(<i>tert</i> -Butyl)-2-methoxybenzene	> 100	> 100		21 4-(<i>sec</i> -Butoxy)-3-(<i>tert</i> -butyl)phenol	2	>50

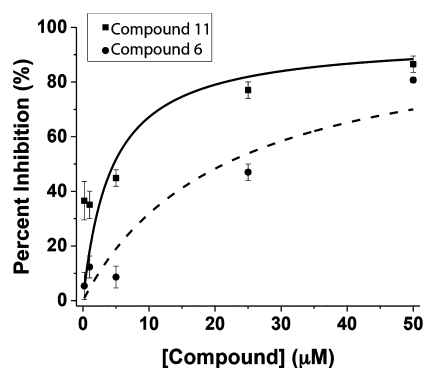


Figure 1. Inhibition of infectious H3 influenza by compounds 6 and 11. For these experiments influenza A (H1N1) virus strain A/Hong Kong/1/1968 infection of A549 cells was used at MOI = 1.0. The data represent an average of experiments performed in triplicates (\pm SD).

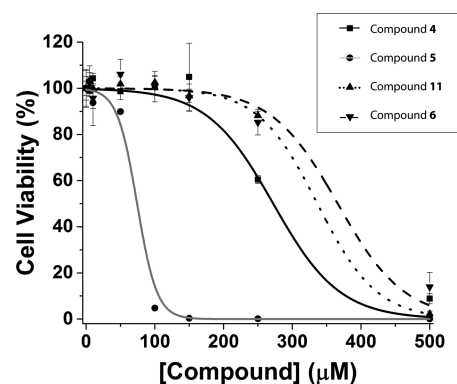


Figure 2. Cytotoxicity of compounds 4, 5, 6, and 11. Three independent experiments were performed with 24 h of incubation using 293T cells.

Biochemical Characterization of the HA Interaction with Compound 11. The reactivity of TBHQ has historically

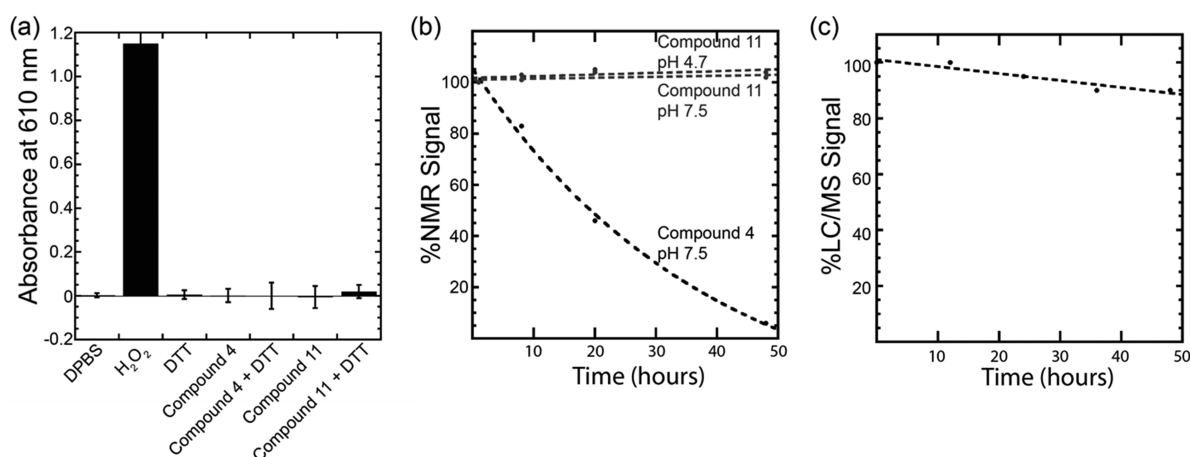


Figure 3. Stability of select compounds. (a) Redox liability of compounds 4 and 11 measured by the method of Johnston et al.³⁴ Experimental conditions were 200 μ M compound, \pm 1 mM DTT, 0.1 mg/mL of Phenol red, and 60 μ g/mL of horseradish peroxidase at room temperature in DPBS. (b) Stability of compounds 4 and 11 as measured by NMR spectroscopy. The stability was assayed by the height of the *tert*-butyl signal in the NMR spectrum under aerobic conditions at pH 7.5 and 4.7. Experimental conditions were 200 μ M compound in 20 mM phosphate/pH 7.5 and 150 mM NaCl or 20 mM D-acetate/pH 4.7 and 150 mM NaCl at 25 $^{\circ}$ C. (c) Stability of compound 11 in DPBS assay buffer as measured by LC-MS.

reduced enthusiasm for its use as a structural template for the development of novel inhibitors of influenza entry. However, we reasoned that substitution of the hydroxyl group by a methoxy group would greatly reduce the compound's reactivity. To first compare the redox liability of compound 11 to that of TBHQ (compound 4), we measured the production of H₂O₂ in the presence of compound using a horseradish peroxidase–phenol red assay.³³ As shown in Figure 3a, compounds 4 and 11 generate very little H₂O₂ over the standard assay time of 2 h, suggesting relatively low amounts of redox activity. To further assay redox liability over a longer time scale, we used a simple NMR assay. As shown in Figure 3b we observe that ~50% of TBHQ (compound 4) is oxidized at 20 h. Interestingly, the oxidation is inhibited by low pH (pH 4.7), due to a decreased formation of phenoxide ions, the main precursor in the oxidation process. These results suggest that TBHQ and other compounds from this series will display increased stability in cell endosomes, which are the primary entry vehicles for influenza and the place where fusion process occurs. On the other hand, compound 11 exhibits little oxidation at 20 h at both pH 7.5 and 4.7, and thus concerns about reactivity are significantly reduced. Finally, we assayed the stability of compound 11 in cell culture buffer by LC-MS. As shown in Figure 3c, compound 11 is highly stable under these conditions.

As discussed above, the binding site of TBHQ is known from the X-ray structure of TBHQ in complex with H3 HA.²² In the next step we confirmed that compound 11 binds to the same site as TBHQ, the parent compound, using a NMR-based competition assay previously developed by our group.^{28,34} As shown in Figure 4, compound 11 displaces TBHQ, verifying that both compounds bind to overlapping sites on H7 HA. On the other hand, compound 5, the oxidized version of TBHQ, exhibits little ability to displace TBHQ (Figure 4), suggesting significantly lower affinity and underscoring the importance of one or more of the hydroxyl groups. Previously, we have characterized the binding mode of TBHQ (compound 4) using STD NMR, which gives insight into the relative distance of ligand ¹H to the protein surface ¹H and can be used to guide chemical optimization.²⁷ Accordingly, we characterized the binding mode of compound 11 by STD. As shown in Figure 5, the ¹H of the methyl group of the anisole makes relatively

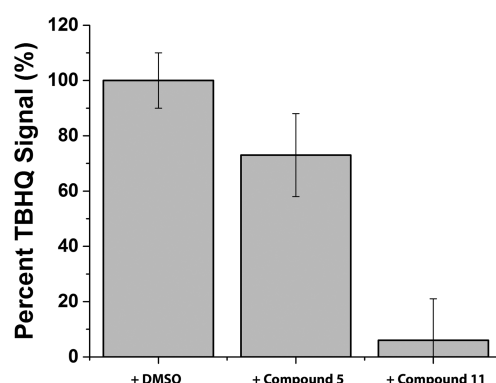


Figure 4. WaterLOGSY competition assay for binding of TBHQ (compound 4) in the presence of compound 11. Compound 5, the oxidized version of TBHQ, is shown as a control. The total length of each experiment was ~2 h. Buffer conditions were 50 mM phosphate/pH 8.2, 50 mM NaCl, and 10% ²H₂O.

extensive contact with the HA surface, which may result in higher affinity and more potent antiviral activity.

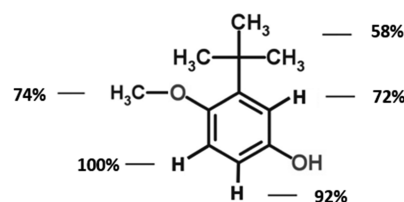


Figure 5. Relative STD signals of compound 11 in the presence of H7 HA. The total length of each STD experiment was ~13 h. Buffer conditions were 50 mM phosphate/pH 8.2, 50 mM NaCl, and 100% ²H₂O.

Molecular Modeling of Interactions with H7 HA. In a next step, we used 10 ns molecular dynamic simulation (MDS) trajectories to analyze the interaction patterns for several compounds of this series with the HA stem loop region of H7 HA. As shown in Figure 6a, the model predicts that the 1-OH and 4-OH groups of TBHQ (compound 4) form hydrogen bonds with the HA2-R54 main chain and the HA2-E97 side

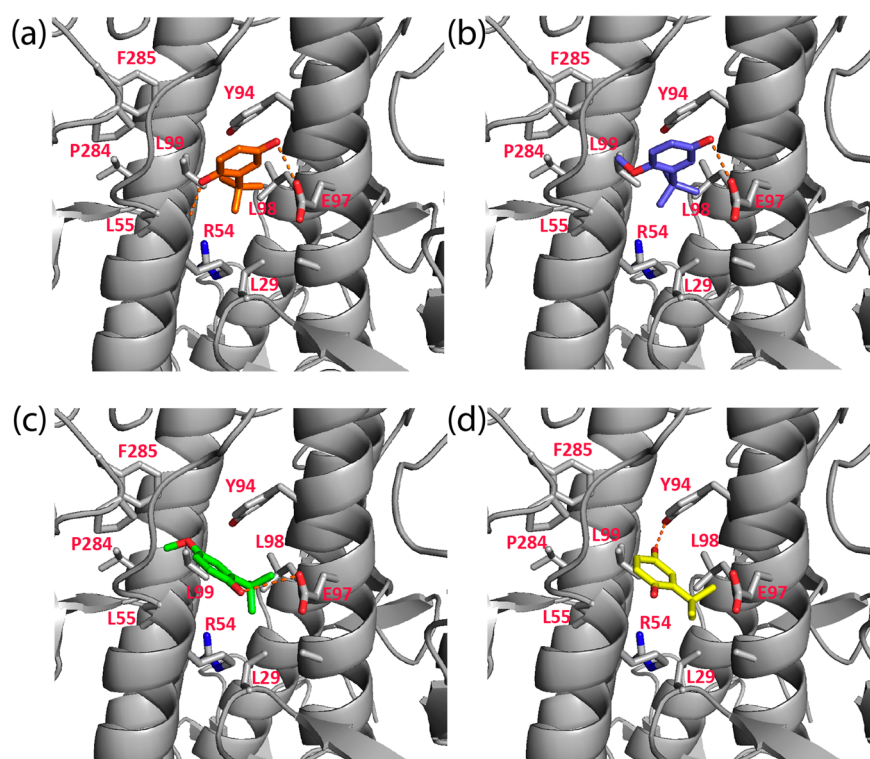


Figure 6. Molecular dynamics models of compounds with H7 HA highlighting important hydrogen bonding and hydrophobic interactions. The models shown include compound 4 (a), compound 11 (b), compound 6 (c), and compound 5 (d). Hydrogen bonding and hydrophobic contacts have been defined as <4 Å distance between appropriate heavy atoms.

chain, respectively. In addition, the *tert*-butyl group forms hydrophobic interactions with the side chains of HA2-L55, HA2-L98, and HA2-L99 (Figure 6a). In the case of our most active compound (compound 11), the model predicts an almost identical orientation of the aromatic ring and *tert*-butyl groups with the most significant difference being the addition of hydrophobic interactions between the 1-methoxy group and the side chains of HA1-P284, HA1-F285, HA2-L55, and HA2-L99 (Figure 6b). In contrast, the predicted binding mode of compound 6, a relatively inactive derivative of TBHQ, is very different. Specifically, the model predicts that the 1-OH of this compound forms a hydrogen bond with the HA2-E97 side chain and that the *tert*-butyl group loses the hydrophobic interaction with the HA2-L99 side chain (Figure 6c). Finally, the predicted binding mode of compound 5, another inactive derivative of TBHQ, is again very different. Specifically, the 1-carbonyl loses the ability to hydrogen bond, the oxygen atom of the carbonyl group having a repulsive interaction with the oxygen of the hydroxyl side chain of HA2-Y94 residue, and the *tert*-butyl group loses hydrophobic interactions with the side chains of HA2-L55 and HA2-L99 (Figure 6d).

Concluding Remarks. In this work we have established that the antioxidant properties of TBHQ are not responsible for the compound's antiviral activity against influenza containing group 2 HA. In addition, we have shown that the 1-hydroxyl forms a critical contact with HA and that the 4-hydroxyl may be modified to improve the IC_{50} to $\sim 0.6 \mu M$, achieve a therapeutic index of >500, and greatly reduce chemical reactivity. Together we feel that these results will renew interest in hydroquinone-based lead compounds as influenza antivirals. Importantly, the present results may encourage previously discarded compounds categorized as PAINS^{30,31} to be re-evaluated with their anisole derivatives to become PAINless.

MATERIALS AND METHODS

Chemicals. Ascorbic acid (compound 1), propyl gallate (compound 2), 2,6-di-*tert*-butyl-4-methylphenol (compound 3), TBHQ (compound 4), and TBBQ (compound 5) were purchased from Sigma. 2-*tert*-Butyl-4-methoxyphenol (compound 6) was purchased from Fluka. 2-*tert*-Butylphenol (compound 7) was purchased from Fisher. 2-*tert*-Butyl-4-methylphenol (compound 8), 2-*tert*-butyl-4-ethylphenol (compound 9), and 4-bromo-2-*tert*-butylphenol (compound 10) were purchased from Enamine. 3-*tert*-Butyl-4-methoxyphenol (compound 11) was purchased from USP. 2-*tert*-Butylanisole (compound 12), 3-*tert*-butyl-4-methoxybenzoic acid (compound 13), (3-(*tert*-butyl)-4-methoxyphenyl)methanol (compound 14), 3-*tert*-butyl-4-methoxybenzamide (compound 15), 3-*tert*-butyl-4-methoxy-*N*-methylbenzamide (compound 16), 3-*tert*-butyl-4-methoxybenzylamine (compound 17), 3-(*tert*-butyl)-4-ethoxyphenol (compound 18), 3-(*tert*-butyl)-4-isopropoxyphenol (compound 19), 3-(*tert*-butyl)-4-isobutoxyphenol (compound 20), and 4-(*sec*-butoxy)-3-(*tert*-butyl)phenol (compound 21) were synthesized in-house as described in the Supporting Information. The purity and identity of all compounds was confirmed by 1D ¹H and ¹³C NMR spectroscopy and LC-MS as described in the Supporting Information.

Antiviral and Cytotoxicity Assays. The pseudovirus entry assays and cytotoxicity assays were performed as previously described.²⁷ Briefly, plasmids pHA-H7 (bearing the HA for strains A/Netherlands/219/2003), pNA (bearing influenza neuraminidase), and pNL4-3.Luc.R-E- were cotransfected by PEI (PolySciences, Inc., Warrington, PA, USA) into 293T cells, which were maintained in Dulbecco's medium with 10% FBS and 1% penicillin–streptomycin. Forty-eight hours post-

transfection, the medium was harvested and filtered through a 0.45 μm filter to make the virus stock. For assay of viral entry, HEK293T cells, which were maintained in Dulbecco's medium with 10% FBS supplemented with 1% penicillin–streptomycin, were seeded to 3×10^4 cells/well of a 24-well cell culture plate in a volume of 0.5 mL. The following day, 500 μL of the virus stock was added to each of the wells of the HEK293T cells after removal of the medium. In experiments with compounds, the pseudovirions were premixed with the appropriate amount of compound from a DMSO stock solution (dilutions of 1:200). The plates were incubated at 37 °C in a CO₂ incubator. After approximately 5–8 h, the virus was aspirated and replaced with cell medium, and the cells were allowed to rest for another 40 h. Luciferase activity was measured using the Luciferase Assay System from Promega (Madison, WI, USA) and a Berthold FB12 luminometer running Sirius software. The experiments were run in triplicate from transfection to assay of luciferase activity, and thus the uncertainties represent all stages of the experiment. In all cases, the viral entry levels fell within the linear range of detection (i.e., the values of the wild-type and mutants never exceeded 1×10^7 relative light units³⁵). Infectious virus assays were performed as previously described.³⁶ Briefly, A549 cells were seeded at a density of 4×10^5 cells/well of a 12-well plate a day prior to infection. The next day, A549 cells were washed twice with PBS and infected with A/Hong Kong/1/1968 (H3N2) at a multiplicity of infection of 1 for 1 h at 37 °C with shaking every 15 min. The infected cells were washed three times with PBS and incubated in DMEM/10% FBS media for 3 h at 37 °C. At 3 h post-infection, the cells were trypsinized and stained with an anti-NP monoclonal antibody followed by Alexa-647 conjugated secondary antibody. The cells were subjected to analysis in an LSRII flow cytometer, and the samples were processed using FlowJo software (TreeStar). The relative inhibition of virus infection was calculated on the basis of DMSO-treated cells. Cytotoxicity was determined using the CellTiter-Glo kit (Promega) after 24 h of incubation of the compounds with 293T cells.

Redox Liability Experiments. Redox liability of select compounds was performed as previously described.³³ Briefly, solutions of 200 μM compound (or equivalent amount of DMSO for the control) were incubated with or without 1 mM DTT, in DPBS media (Corning), for 2 h at room temperature. Total sample volume was 0.95 mL (the remaining 50 μL was left for the addition of other reagents). After 2 h, a reaction mixture of horseradish peroxidase (HRP)–phenol red was added to each sample. Final concentrations were 0.1 mg/mL phenol red and 60 $\mu\text{g/mL}$ HRP. Following 45 min of incubation at room temperature, the reactions were stopped by the addition of 0.15 N KOH (final concentration). Absorbance at 610 nm was used to measure the amount of generated H₂O₂ using 0.1 mg/mL solution of phenol red as the blank. A 100 μM solution of H₂O₂ (with the reaction mixture) was used as a positive control. Experiments were performed in triplicate.

WaterLOGSY and STD NMR Experiments. NMR experiments were performed on Bruker 800 or 900 MHz AVANCE spectrometers equipped with room temperature or cryogenic triple-resonance probes, respectively, at 25 °C. Recombinant H7 HA was obtained from BEI Resources. WL experiments were performed as previously described.³⁷ To saturate water ¹H, 2 ms square-shaped pulses were used and the total saturation time was 2 s with a relaxation delay of 2.5 s. The

number of scans was set to 1024, which corresponds to a ~ 2 h experiment. The WL competition experiments were performed with 0.5 μM HA, 50 μM TBHQ (compound 4), and 500 μM compound 11 (or DMSO control) in 20 mM phosphate buffer, pH 7.2, with 150 mM NaCl. Saturation transfer difference (STD) experiments were performed as previously described.³⁷ A train of 50 ms Gaussian pulses was used to selectively excite the protein ¹H. Total saturation time was 1 s, and the relaxation delay was set to 2.5 s. “On” resonance frequency was set to -0.5 ppm, and the “off” resonance acquisition was set to 50 ppm. The total length of each STD experiment was ~ 13 h. Buffer conditions were 50 mM phosphate, pH 8.2, 50 mM NaCl, and 10% ²H₂O for WL or 100% ²H₂O for STD. Three millimeter NMR tubes were used in all studies. Data were processed and analyzed using NMRDraw.³⁸ Relative percent STD was calculated as described previously.³⁴ Briefly, % STD = $100 \times \text{STD}_{\text{obs}}/\text{STD}_{\text{max}}$. STD signal was calculated according to the equation $\text{STD} = \Delta I/I_{\text{off}}$ where $\Delta I = I_{\text{off}} - I_{\text{on}}$, and I_{off} and I_{on} are the resonance intensities after the “off” and “on” presaturation of the protein/VLP target. Errors in STD experiments were estimated as $\Delta I/I_{\text{ref}}((N_{\Delta I}/\Delta I)^2 + (N_{\text{ref}}/I_{\text{ref}})^2)^{0.5}$, where $N_{\Delta I}$ and N_{ref} are the noise levels calculated by NMRDraw in the appropriate spectrum.

Molecular Modeling. The crystal structure of the H7 (4R8W.pdb) was considered for the modeling studies. In this crystal structure the H7 HA is complexed with antibody CT149. To consider the H7 structure, we deleted the antibody part from the complex. The monomer crystal structure was considered to build the trimer structure of H7. Using the homomultimer building tools implemented in the Schrodinger platform (Schrodinger 2014-4: Prime, version 3.8, Schrödinger, LLC) with the reference structure of 3EYM.pdb (H3 HA complexed with TBHQ), the trimer structure of H7 HA was built. The SITE-ID module of Tripos molecular modeling package (SybylX 1.3; Tripos International) was used to identify the potential small molecule ligand binding sites in the trimer structure of H7 HA. Superposing the trimer structure of H7 HA with the trimer structure of H3 HA complexed with TBHQ, we observed that the small molecule binding sites of both H7 and H3 HAs exhibit 84% similar residues. The FlexiDock docking package of Tripos was used to pre-position ligands (compounds 4 and 11) in the identified ligand binding site of H7 HA. FlexiDock works in torsional space, keeping the bond lengths and angles constant while allowing the amino acids interacting with the ligand to be flexible during the docking process. The energetically most favorable position and the pose of the ligand obtained from FlexiDock was considered for further modeling studies. The MDS in optimized potentials for liquid simulations (OPLS2005) force field was used to carry out the MDS of the H7 HA and the ligand complex structures. All of the MDS computations were carried out in MacroModel 9.8 implemented in Schrodinger software suite (MacroModel 9.8, Schrodinger, LLC) in one NPT ensemble (constant number of molecules, pressure, and temperature). In the MacroModel dynamics panel, stochastic dynamics was chosen as it includes random forces that stimulate the buffering of a system by solvent molecules. To constrain the bond lengths to the original values, the “SHAKE” option was selected. The simulation of the complex was carried out at 300 K with a time step of 1.5 fs and equilibrium time of 1 ps. The MDS was run for 1, 5, and 10 ns by recording the energies and the trajectories of the system. The plot of the potential energy versus the time

at 10 ns revealed that the system had attained an equilibrium condition.

■ ASSOCIATED CONTENT

■ Supporting Information

The Supporting Information is available free of charge on the ACS Publications website at DOI: [10.1021/acsinfecdis.6b00046](https://doi.org/10.1021/acsinfecdis.6b00046).

Synthesis methods and 1D ^1H and ^{13}C NMR spectra (PDF)

■ AUTHOR INFORMATION

Corresponding Author

*(M.C.) E-mail: caffrey@uic.edu.

Notes

The authors declare no competing financial interest.

■ ACKNOWLEDGMENTS

This research was supported by DHHS/NIH Grant R21AI101676 and the Chicago Biomedical Consortium with support from the Searle Funds at the Chicago Community Trust. We thank the Herbert E. Paaren Endowment for Chemical Sciences for generous support in the form of a Paaren Fellowship to N.J.H.

■ REFERENCES

- (1) Skehel, J. J., and Wiley, D. C. (2000) Receptor binding and membrane fusion in virus entry: the influenza hemagglutinin. *Annu. Rev. Biochem.* 69, 531–569.
- (2) Webster, R. G., Bean, W. J., Gorman, O. T., Chambers, T. M., and Kawaoka, Y. (1992) Evolution and ecology of influenza A viruses. *Microbiol. Rev.* 56, 152–179.
- (3) Johnson, N. P., and Mueller, J. (2002) Updating the accounts: global mortality of the 1918–1920 “Spanish” influenza pandemic. *Bull. Hist. Med.* 76, 105–115.
- (4) Ginsberg, J., Mohebbi, M. H., Patel, R. S., Brammer, L., Smolinski, M. S., and Brilliant, L. (2009) Detecting influenza epidemics using search engine query data. *Nature* 457, 1012–1014.
- (5) Chen, Y., Liang, W., Yang, S., Wu, N., Gao, H., Sheng, J., Yao, H., Wo, J., Fang, Q., Cui, D., Li, Y., Yao, X., Zhang, Y., Wu, H., Zheng, S., Diao, H., Xia, S., Zhang, Y., Chan, K. H., Tsoi, H. W., Teng, J. L., Song, W., Wang, P., Lau, S. Y., Zheng, M., Chan, J. F., To, K. K., Chen, H., Li, L., and Yuen, K. Y. (2013) Human infections with the emerging avian influenza A H7N9 virus from wet market poultry: clinical analysis and characterisation of viral genome. *Lancet* 381, 1916–1925.
- (6) Gao, R., Cao, B., Hu, Y., Feng, Z., Wang, D., Hu, W., Chen, J., Jie, Z., Qiu, H., Xu, K., Xu, X., Lu, H., Zhu, W., Gao, Z., Xiang, N., Shen, Y., He, Z., Gu, Y., Zhang, Z., Yang, Y., Zhao, X., Zhou, L., Li, X., Zou, S., Zhang, Y., Li, X., Yang, L., Guo, J., Dong, J., Li, Q., Dong, L., Zhu, Y., Bai, T., Wang, S., Hao, P., Yang, W., Zhang, Y., Han, J., Yu, H., Li, D., Gao, G. F., Wu, G., Wang, Y., Yuan, Z., and Shu, Y. (2013) Human infection with a novel avian-origin influenza A (H7N9) virus. *N. Engl. J. Med.* 368, 1888–1897.
- (7) Lagoja, I. M., and De Clercq, E. (2008) Anti-influenza virus agents: synthesis and mode of action. *Med. Res. Rev.* 28, 1–38.
- (8) van der Vries, E., Stelma, F. F., and Boucher, C. A. (2010) Emergence of a multidrug-resistant pandemic influenza A (H1N1) virus. *N. Engl. J. Med.* 363, 1381–1382.
- (9) Marjuki, H., Mishin, V. P., Chesnokov, A. P., Jones, J., De La Cruz, J. A., Sleeman, K., Tamura, D., Nguyen, H. T., Wu, H. S., Chang, F. Y., Liu, M. T., Fry, A. M., Cox, N. J., Villanueva, J. M., Davis, C. T., and Gubareva, L. V. (2015) Characterization of drug-resistant influenza A (H7N9) variants isolated from an Oseltamivir-treated patient in Taiwan. *J. Infect. Dis.* 211, 249–257.
- (10) Eckert, D. M., and Kim, P. S. (2001) Mechanisms of viral membrane fusion and its inhibition. *Annu. Rev. Biochem.* 70, 777–810.
- (11) Harrison, S. C. (2008) Viral membrane fusion. *Nat. Struct. Mol. Biol.* 15, 690–698.
- (12) Caffrey, M. (2011) HIV envelope: challenges and opportunities for the discovery of entry inhibitors. *Trends Microbiol.* 19, 191–197.
- (13) Belouzard, S., Millet, J. K., Licitra, B. N., and Whittaker, G. R. (2012) Mechanisms of coronavirus cell entry mediated by the viral spike protein. *Viruses* 4, 1011–1033.
- (14) Nobusawa, E., Aoyama, T., Kato, H., Suzuki, Y., Tateno, Y., and Nakajima, K. (1991) Comparison of complete amino acid sequences and receptor-binding properties among 13 serotypes of hemagglutinins of influenza A viruses. *Virology* 182, 475–485.
- (15) Bodian, D. L., Yamasaki, R. B., Buswell, R. L., Stearns, J. F., White, J. M., and Kuntz, I. D. (1993) Inhibition of the fusion-inducing conformational change of influenza hemagglutinin by benzoquinones and hydroquinones. *Biochemistry* 32, 2967–2978.
- (16) Hoffman, L. R., Kuntz, I. D., and White, J. M. (1997) Structure-based identification of an inducer of the low-pH conformational change in the influenza virus hemagglutinin: irreversible inhibition of infectivity. *J. Virol.* 71, 8808–8820.
- (17) Staschke, K. A., Hatch, S. D., Tang, J. C., Hornback, W. J., Munroe, J. E., Colacino, J. M., and Muesing, M. A. (1998) Inhibition of influenza virus hemagglutinin-mediated membrane fusion by a compound related to podocarpic acid. *Virology* 248, 264–274.
- (18) Cianci, C., Yu, K. L., Dischino, D. D., Harte, W., Deshpande, M., Luo, G., Colonna, R. J., Meanwell, N. A., and Krystal, M. (1999) pH-dependent changes in photoaffinity labeling patterns of the H1 influenza virus hemagglutinin by using an inhibitor of viral fusion. *J. Virol.* 73, 1785–1794.
- (19) Oka, M., Ishiwata, Y., Iwata, N., Honda, N., and Kakigami, T. (2001) Synthesis and anti-influenza virus activity of tricyclic compounds with a unique amine moiety. *Chem. Pharm. Bull.* 49, 379–383.
- (20) Deshpande, M. S., Wei, J., Luo, G., Cianci, C., Danetz, S., Torri, A., Tiley, L., Krystal, M., Yu, K. L., Huang, S., Gao, Q., and Meanwell, N. A. (2001) An approach to the identification of potent inhibitors of influenza virus fusion using parallel synthesis methodology. *Bioorg. Med. Chem. Lett.* 11, 2393–2396.
- (21) Yu, K. L., Torri, A. F., Luo, G., Cianci, C., Grant-Young, K., Danetz, S., Tiley, L., Krystal, M., and Meanwell, N. A. (2002) Structure-activity relationships for a series of thiobenzamide influenza fusion inhibitors derived from 1,3,3-trimethyl-5-hydroxy-cyclohexyl-methylamine. *Bioorg. Med. Chem. Lett.* 12, 3379–3382.
- (22) Russell, R. J., Kerry, P. S., Stevens, D. J., Steinhauer, D. A., Martin, S. R., Gamblin, S. J., and Skehel, J. J. (2008) Structure of influenza hemagglutinin in complex with an inhibitor of membrane fusion. *Proc. Natl. Acad. Sci. U. S. A.* 105, 17736–17741.
- (23) Han, T., and Marasco, W. A. (2011) Structural basis of influenza virus neutralization. *Ann. N. Y. Acad. Sci.* 1217, 178–190.
- (24) Fleishman, S. J., Whitehead, T. A., Ekiert, D. C., Dreyfus, C., Corn, J. E., Strauch, E. M., Wilson, I. A., and Baker, D. (2011) Computational design of proteins targeting the conserved stem region of influenza hemagglutinin. *Science* 332, 816–821.
- (25) Ekiert, D. C., Friesen, R. H., Bhabha, G., Kwaks, T., Jongeneelen, M., Yu, W., Ophorst, C., Cox, F., Korse, H. J., Brandenburg, B., Vogels, R., Brakenhoff, J. P., Kompier, R., Koldijk, M. H., Cornelissen, L. A., Poon, L. L., Peiris, M., Koudstaal, W., Wilson, I. A., and Goudsmit, J. (2011) A highly conserved neutralizing epitope on group 2 influenza A viruses. *Science* 333, 843–850.
- (26) Dreyfus, C., Ekiert, D. C., and Wilson, I. A. (2013) Structure of a classical broadly neutralizing stem antibody in complex with a pandemic H2 hemagglutinin. *J. Virol.* 87, 7149–7154.
- (27) Antanasijevic, A., Cheng, H., Wardrop, D. J., Rong, L., and Caffrey, M. (2013) Inhibition of influenza H7 hemagglutinin-mediated entry. *PLoS One* 8 (10), e76363.
- (28) Basu, A., Antanasijevic, A., Wang, M., Li, B., Mills, D., Ames, J., Moir, D. T., Prichard, M., Barnard, D. L., Caffrey, M., Rong, L., and

Bowlin, T. L. (2014) Novel inhibitors of influenza A virus fusion: interaction with the viral hemagglutinin. *J. Virol.* 88, 1447–1460.

(29) van Esch, G. J. (1986) Toxicology of *tert*-butylhydroquinone (TBHQ). *Food Chem. Toxicol.* 24, 1063–1065.

(30) Baell, J. B., and Holloway, G. A. (2010) New substructure filters for removal of pan assay interference compounds (PAINS) from screening libraries and for their exclusion in bioassays. *J. Med. Chem.* 53, 2719–2740.

(31) Dahlin, J. L., and Walters, M. A. (2016) How to triage PAINS-full research. *Assay Drug Dev. Technol.* 14, 168–174.

(32) Ooi, N., Chopra, I., Eady, A., Cove, J., Bojar, R., and O'Neill, A. J. (2013) Antibacterial activity and mode of action of *tert*-butylhydroquinone (TBHQ) and its oxidation product, *tert*-butylbenzoquinone (TBBQ). *J. Antimicrob. Chemother.* 68, 1297–304.

(33) Johnston, P. A., Soares, K. M., Shinde, S. N., Foster, C. A., Shun, T. Y., Takyi, H. K., Wipf, P., and Lazo, J. S. (2008) Development of a 384-well colorimetric assay to quantify hydrogen peroxide generated by the redox cycling of compounds in the presence of reducing agents. *Assay Drug Dev. Technol.* 6, 505–518.

(34) McCullough, C., Wang, M., Rong, L., and Caffrey, M. (2012) Characterization of influenza hemagglutinin interactions with receptor by NMR. *PLoS One* 7, e33958.

(35) Wang, J., Sen, J., Rong, L., and Caffrey, M. (2008) Role of the HIV gp120 conserved domain 1 in processing and viral entry. *J. Biol. Chem.* 283, 32644–32649.

(36) Manicassamy, B., Medina, R. A., Hai, R., Tsibane, T., Stertz, S., Nistal-Villán, E., Palese, P., Basler, C. F., and García-Sastre, A. (2010) Protection of mice against lethal challenge with 2009 H1N1 influenza A virus by 1918-like and classical swine H1N1 based vaccines. *PLoS Pathog.* 6 (1), e1000745.

(37) Antanasijevic, A., Ramirez, B., and Caffrey, M. (2014) Comparison of the sensitivities of WaterLOGSY and saturation transfer difference NMR experiments. *J. Biomol. NMR* 60, 37–44.

(38) Delaglio, F., Grzesiek, S., Vuister, G. W., Zhu, G., Pfeifer, J., and Bax, A. (1995) NMRPipe: a multidimensional spectral processing system based on UNIX pipes. *J. Biomol. NMR* 6, 277–293.